



Eidgenössische Technische Hochschule Zürich
Swiss Federal Institute of Technology Zurich

Agent-Based Modeling and Social System Simulation
Project Report

**Modelling the outbreak of an influenza strain in
a population with different belief groups**

Antunes Morgado, Nicolas; Gundersen, Benjamin;
Hühnerbein, Jannes & Siebenaller, Julius

Zürich
Fall Semester 2019



Eidgenössische Technische Hochschule Zürich
Swiss Federal Institute of Technology Zurich

Declaration of originality

The signed declaration of originality is a component of every semester paper, Bachelor's thesis, Master's thesis and any other degree paper undertaken during the course of studies, including the respective electronic versions.

Lecturers may also require a declaration of originality for other written papers compiled for their courses.

I hereby confirm that I am the sole author of the written work here enclosed and that I have compiled it in my own words. Parts excepted are corrections of form and content by the supervisor.

Title of work (in block letters):

Modelling the outbreak of an influenza strain in a population with different belief groups

Authored by (in block letters):

For papers written by groups the names of all authors are required.

Name(s):

Gundersen
Siebenaller
ANTONIO MORENO
Hühnerbein

First name(s):

Benjamin
Julius
NICOLAS GABRIEL
Yannès

With my signature I confirm that

- I have committed none of the forms of plagiarism described in the 'Citation etiquette' information sheet.
- I have documented all methods, data and processes truthfully.
- I have not manipulated any data.
- I have mentioned all persons who were significant facilitators of the work.

I am aware that the work may be screened electronically for plagiarism.

Place, date

Zürich, 2.12. 2019

Signature(s)

Benjamin Gundersen
Julius Siebenaller
Yannès Hühnerbein

For papers written by groups the names of all authors are required. Their signatures collectively guarantee the entire content of the written paper.

Agreement for free-download

We hereby agree to make our source code for this project freely available for download from the web pages of the Computational Social Science chair. Furthermore, we assure that all source code is written by ourselves and is not violating any copyright restrictions.

Nicolas Antunes Morgado

Benjamin Gundersen

Jannes Hühnerbein

Julius Siebenaller

Modelling the outbreak of an influenza strain in a population with different belief groups

Antunes Morgado, Nicolas; Gundersen, Benjamin;
Hühnerbein, Jannes; Siebenaller, Julius

Abstract

In this thesis, the outbreak of an influenza strain is modelled for a community that consists of two belief groups regarding vaccination ('Trusters' and 'Skepticals' with different costs of vaccination). Both groups form sub-groups of the community and are assumed to resemble small-world networks, which are further combined.

Relying on an SIVR-model, the spread of the disease is according to the infection rate and the decisions of the individual agents. The agents follow a simple game theoretical model in order to arrive at a decision to vaccinate, taking into account the forecast for a certain period, which is updated regularly.

The main emphasis is being placed on investigating different distributions of the communities and the effect this has on the disease outbreak. Besides, the outcomes of changing the agent-specific parameters, costs of vaccination, costs of infection and time-horizon, are analysed as well. The results are in line with and confirm previous research. But especially, it is obtained that uptake levels are more sensitive to the share of trusters in the community, compared to the cost-ratios of the individual communities.

Individual contributions

The authors have contributed equally to this thesis.

Contents

1	Introduction and Motivations	5
2	Literature Review	6
3	Description of the Model	8
3.1	Epidemic dynamics	10
3.2	Agent policy	10
3.3	Network structure	13
4	Initial Setup and Baseline Parameters	14
5	Implementation	14
5.1	Creating the network	15
5.2	Simulating the agents' behaviour	15
6	Simulation Results and Discussion	16
7	Summary and Outlook	17
	Appendix	19
	References	23

1 Introduction and Motivations

Several times in human history epidemics have left areas and sometimes entire civilisations in total devastation. Only with the rise of modern medicine and especially widely available vaccines the development of large and complex societies of today was made possible.

The characteristics of the flu with its almost yearly outbreaks and frequent mutations - making a general vaccine impossible to develop - yield an interesting game theoretical problem. While vaccinations are quickly developed, the uptake levels of vaccines is crucial regarding the spread and containment of an outbreak. With 'anti-vaccination' groups becoming more and more popular and diseases thought to be extinct reappearing even in Central Europe, the effects on disease outbreaks are gaining relevance and needs to be analysed in more detail.

Previous works in epidemiology have developed models to capture disease dynamics in various population structures. While another strand of literature has turned to a game-theoretical perspective to extensively analyse the decision process of an individual on the uptake of vaccination.

In this thesis, the outbreak of an influenza strain is modelled for a community that consists of two belief groups regarding vaccination. One is trusting the effectiveness and safety of vaccines and assumes a lower cost to vaccination. The other group is skeptical towards vaccinations. Both groups form sub-groups of the community and are assumed to resemble small-world networks. These networks are further combined to form the whole population. Relying on an SIVR-model, the spread of the disease is according to the infection rate and the decisions of the individual agents. The agents follow a simple game theoretical model in order to arrive at a decision to vaccinate, taken into account the forecast for a certain period. The decision is update regularly. The time-horizon taken into account is for one single flu season. The main emphasis is being placed on investigating different distributions of the communities and the effect this has on the disease outbreak. Besides, the outcomes of changing the agent-specific parameters, costs of vaccination, costs of infection and time-horizon, are analysed as well. The results are in line with and confirm previous research. Of particular interest is the comparison of the effect of the share of trusters to the different cost-ratios in the two belief groups.

The thesis is organised as follows: [Section 2](#) reviews the relevant literature on modelling of infectious diseases and the game theoretical analysis of the vaccination decision. [Section 3](#) describes the model, including epidemic dynamics, agent policy and network structure. The initial setup and baseline parameters are provided in [Section 4](#) and [Section 5](#) deals with the implementation. [Section 6](#) describes the results with a discussion of the findings. [Section 7](#) concludes.

2 Literature Review

The following provides a small review of the literature concerning (1) the modelling of infectious diseases with respect to population structures and subpopulations as well as disease spreading. And (2) a game theoretical analysis regarding the vaccination decisions of individuals.

The work of [Kermack and McKendrick \(1927\)](#) is pivotal in the field of epidemiology, particularly concerning the spread of an infectious disease in a population. Susceptible persons get infected based on the transmission rate of the disease and the size of the infectious subpopulation. They finally recover or die from the disease and hence join and stay in the recovered pool. This and subsequent compartmental models are commonly referred to as SIR-models of infectious diseases. As outlined in [Earn et al. \(2008\)](#), respectively in [Dadlani \(2013\)](#) or [Sun et al. \(2016\)](#), there exist various adaptations of the SIR-compartmental-model to either allow for different subpopulations, or to modify the disease process.¹

Underlying these compartmental models is the mass-action assumption, meaning that a homogeneous population is assumed in which all individuals are connected ([Heesterbeek, 2005](#); [Rusu, 2015](#); [Wilson and Worcester, 1945](#)). These limitations have been tackled by working with networks which allow to weaken the mass-action assumption, thus providing a better fit for the combination of population structures and disease transmissions ([Keeling and Eames, 2005](#); [Meyers et al., 2005](#)).²

A strand of literature has been published regarding the influence of the network structure on the percolation of the disease, meaning the spread of the infectious disease in the population. In particular, attention has been put on analysing and calculation the percolation threshold for different population structures. Concerning small-world networks, the deduction of the epidemic threshold, for both bond and site percolation, can be found in prior works of [Newman and Watts \(1999\)](#) and [Moore and Newman \(2000\)](#). The network structure is decisive for the epidemic threshold, which determines the onset of an epidemic. For complex networks, [Pastor-Satorras and Vespignani \(2002\)](#) show that eradication of infections cannot be achieved by random uniform immunisation of individuals. Analysing small-world networks, [Liu et al. \(2015\)](#) confirm the crucial effect of network structure on the spreading of an infectious disease.³

¹The case of severe acute respiratory syndrome (SARS) serves as an example to model the infectious disease with an additional exposed subpopulations as an interphase between the susceptible and the infected state (SEI-models). Besides, certain diseases do not allow permanent recovery and the person affected joins the susceptible pool again. Examples include gonorrhoea or encephalitis, which are represented in SIS-models and do not comprise a recovered pool, or for instance the seasonality of influenza is represented in SIRS-models ([Dadlani, 2013](#)).

²Network models that are commonly utilised include random networks, lattices, small-world or scale-free networks, amongst others ([Keeling and Eames, 2005](#)).

³[Liu et al. \(2015\)](#) work with small-world networks that are created by randomly dis- and reconnecting the edges in two lattice-structures. Especially for a smaller infection rate, reducing the distances of the

Not only have network structures a significant impact on the range and transmission of an infectious disease, but they enable a shift in perspective to focus more on the individual agent with the related neighbourhood. Analysing the individual agent by adopting a game-theoretical perspective, the calculation of payoffs from vaccination and infection are of significance.

Starting with the simple game-theoretical model in [Bauch and Earn \(2004\)](#), they find that even minimal risks associated with a vaccination drive the uptake levels below the eradication threshold, given that agents behave selfishly. Introducing evolutionary game-theory with social learning, the work of [Bauch and Bhattacharyya \(2012\)](#) displays that these features allow for a better explanation of the evolution of vaccine-scares, which is further analysed in subsequent works. Analysing groups with different beliefs concerning vaccination decisions has gained further interest. For instance, [Liu et al. \(2012\)](#) find that the presence of committed vaccinators increases uptake of vaccines and avoids clustering of susceptibles for agents relying on adaptive-learning.

Combining the game-theoretical perspective with network structures yields further results that are important for epidemiology. [Fu et al. \(2010\)](#) show that agents forming beliefs by relying on adaptive-learning in complex networks, arrive at sub-optimal vaccination levels, which is exacerbated when the selection of successful strategies is sensitive. Furthermore, the network structure has the potential to increase uptake levels, while it may serve as a catalyst to vaccination refusal for increases in vaccination costs. [Shi et al. \(2017\)](#) examine the effects of complex network structures on individual vaccine uptake in mixed strategies. Given an increase of the relative costs of vaccination, they find that heterogenous network structures preserve vaccination rates when compared to regular networks. Moreover, if only direct neighbours are considered, highly connected individuals are likelier to vaccinate, compared to the case of neighbours of neighbours. ([Shi et al., 2017](#))

Especially, the work of [Shim et al. \(2012\)](#) motivates the approach that is employed in this paper. Providing a game-theoretical model of measles transmissions, they analyse the effect of perceived vaccine risks on uptake levels for a population divided into vaccine-sceptics and -believers. It is confirmed that uptake levels are lower if agents behave selfishly, which is more severe for vaccine-sceptics. Moreover, and of particular importance, they show that it is mainly the fraction of vaccine-sceptics, as opposed to their discrepancy in assessing vaccine risks, which drives reduced uptake levels. Especially the last finding is confirmed in [Stegehuis et al. \(2016\)](#). By analysing hierarchical configuration models, formed by connecting communities in networks, this work shows that the mesoscopic set of communities has the main influence on percolations in networks.

networks significantly contributes to a stronger spread of the disease.

3 Description of the Model

The general assumptions of our model are as follows:

- The infectious disease is modelled as a time-homogeneous Markov chain with a finite state space according to an SIVR-process with 'vaccinated', respectively 'recovered' representing the final or absorbing states with permanent immunity. The population is assumed to stay constant.
- Agents are assumed to be rational utility-maximisers endowed with complete information about their immediate neighbourhood. They decide in each time-step whether or not to update their vaccination decision and hence if they will get vaccinated employing a mixed strategy.
- When facing the vaccination decision, each agent samples the health status of its direct neighbours and deduces the probability of infection during the next epoch from the share of infected neighbours.
- The time-horizon of an agent is bounded, in the sense that only a certain amount of time-steps is considered in the calculation of expected utility to be maximised through the vaccination-decision.
- Agents have a group affiliation to either be skeptical (group: 'skepticals') or trust (group: 'trusters') that vaccines are safe. The group membership of an agent determines the subjective costs they assign to vaccination, while the costs of infection are assumed to be equal between groups.
- The population structure is modelled as a small-world network, relying on a Watts-Strogatz model. Two groups are assumed which represent small-worlds on their own. These two networks are then combined assuming that closeness in a group is larger than between groups.

Concerning the epidemiological part of our model, the spread of the disease in the population follows an SIVR-process. Thus, the population is divided into (1) susceptible (2) infectious (3) recovered and (4) vaccinated subpopulations. The subpopulations are the same for the two belief-groups of skepticals and trusters. Susceptible agents can transition to the infectious state, $S \rightarrow I$, by at least one interaction with an infected, hence contagious, neighbour. Individual interactions have probability β of infecting a susceptible agent, while the actual probability of infection $\lambda_k(t)$ depends on the number of infected neighbours. On the other hand, the agent decides to vaccinate with probability $p_{vacc}(t)$ at time-step t and the transition occurs according to the rule $S \rightarrow V$. Infectious agents recover by the probability γ_k with transition $I \rightarrow R$. Recovered, respectively vaccinated, agents stay in their respective state which can be regarded as isomorphic with the exception of how these states are reached. Both recovered and vaccinated agents

are assumed to become fully immunised. A constant population is assumed in a way that no entries, via birth, or exits, via death, are taken into account.⁴

With regards to the agent's decision and infection propagation processes, the work of [Shim et al. \(2012\)](#) motivated the modelling choices, which are partly derived from their analysis. Still, the approach developed in the present work deviates from it in several respects: First off, a discrete-time rather than continuous time Markov process is used to describe disease dynamics. This choice is justified both on simplicity grounds and because at least parts of the mechanism leading to contracting a disease, such as meeting other agents, can be considered inherently discrete events. Secondly, [Shim et al. \(2012\)](#) employ time dependent population balances to derive steady state solutions to an endemic disease (measles), while the decision to vaccinate newborns by their parents has long-term effects. This leads to the explicit modelling of birth-death rates in the population balances and the use of infinitely long time horizons when calculating the agent's expected utilities. The large time scales associated with the decision to vaccinate also give credibility to the assumption of complete knowledge of population-level information, such as the global steady state incidence of measles which is likely available to parents who decide to vaccinate their children. Finally, this game-theoretic setting is sufficient for the existence of a Nash equilibrium which the authors derive for the diverging vaccination policies of different social groups.

In opposition, in the present work it is attempted to describe an infectious disease with short time scales of propagation and recovery, with characteristics of an unexpected outbreak for which a vaccine could be readily available for any individual independently of it's age.⁵ Under these conditions it is not expected to reach an endemic steady state but a mixture of immunised agents, either due to recovery or to vaccination. Moreover, the effective consequences of the decision to vaccinate are assumed to be limited in time, and so agents should only have access to information from their local social links and prior beliefs to evaluate the costs involved. This implies that no Nash equilibrium can arise at the population level, but rather a set of heterogeneous decisions under non-equilibrium conditions. All in all, these are the reasons why birth-death terms in population balances are omitted. Therefore, the time-horizon and knowledge of the infection prevalence to each agent's neighbourhood in the determination of their expected utility is limited, and a network structure for the population rather than a well mixed approximation is relied on.

⁴A more detailed version of the SIVR-model can be found in [Tornatore et al. \(2014\)](#).

⁵An empirical example satisfying the employed definition would be the H1N1 avian flu pandemic of 2009 (cf. [Hancock et al. \(2009\)](#), [Neumann et al. \(2009\)](#), or [Smith et al. \(2009\)](#), amongst others).

3.1 Epidemic dynamics

The evolution of the states of agent k is summarised in the stochastic matrix $\mathbf{Q}_k(t)$ and the health-state probability vector $\mathbf{x}_k(t)$. The disease-specific parameters and transmission rates are outlined below:

$$\mathbf{x}_k(t+1) = \mathbf{Q}_k(t) \cdot \mathbf{x}_k(t) \quad (1)$$

and:

$$\mathbf{Q}_k(t) = \begin{pmatrix} p_k(S \rightarrow S) & p_k(I \rightarrow S) & p_k(R \rightarrow S) & p_k(V \rightarrow S) \\ p_k(S \rightarrow I) & p_k(I \rightarrow I) & p_k(R \rightarrow I) & p_k(V \rightarrow I) \\ p_k(S \rightarrow R) & p_k(I \rightarrow R) & p_k(R \rightarrow R) & p_k(V \rightarrow R) \\ p_k(S \rightarrow V) & p_k(I \rightarrow V) & p_k(R \rightarrow V) & p_k(V \rightarrow V) \end{pmatrix} \quad (2)$$

In particular:

$$\mathbf{Q}_k(t) = \begin{pmatrix} 1 - \lambda_k(t) & 0 & 0 & 0 \\ \lambda_k(t) & 1 - \gamma_k & 0 & 0 \\ 0 & \gamma_k & 1 & 0 \\ 0 & 0 & 0 & 1 \end{pmatrix} \quad (3)$$

For infected agents, the probability of transitioning to a recovered state or remaining infected does not depend on the spread of the disease nor can it be influenced by a decision to vaccinate. Given the absorbing quality of recovered and vaccinated states, this means that only susceptible individuals are active decision makers in the population. For purely susceptible agents, the health probability column vector:

$$\mathbf{x}_k(t)' = (1 - p_{vacc}, 0, 0, p_{vacc}), \quad (4)$$

represents their state at time t after the choice of vaccination strategy.

As outlined above, β represents the probability for an agent of getting infected by a single interaction. This parameter is assumed to be disease-specific, and thus constant in value and independent of the agent's state. The probability of infection $\lambda_k(t)$ for an agent interacting with its entire neighbourhood results:

$$\lambda_k(t) = 1 - (1 - \beta)^{n_k(t)}, \quad (5)$$

with the integer $n_k(t)$ representing the instantaneous number of infected neighbours of agent k at time t .

3.2 Agent policy

A susceptible agent, being a rational utility-maximiser, faces the vaccination decision by solving the optimisation problem:

$$\max_{p_{vacc}} U_k(\mathbf{x}_k(t), T), \quad (6)$$

where T represents the time-horizon of the agent. The expected utility function takes the subsequent form, following the Bellman equation for a discrete-time Markov process:

$$U_k(\mathbf{x}_k(t), T) = \sum_{t'=t}^{t+T} \frac{\mathbf{f}_k(t') \cdot \mathbf{x}_k(t')}{(1+r)^{(t'-t)}}, \quad (7)$$

where $\mathbf{f}_k(t)$ is the payoff row vector of agent k with:

$$\mathbf{f}_k(t' = t) = (0 \quad 0 \quad 0 \quad -C_{v,k}) \quad (8)$$

and:

$$\mathbf{f}_k(t' > t) = (0 \quad -C_{i,k} \quad 0 \quad 0) \quad (9)$$

represent the immediate vaccination payoffs, respectively the payoffs per time step as a result of infection. The different components of the perceived cost, among others the market price of the vaccine and the expected side-effects conditional on the agent's beliefs, are included in $C_{v,k}$. Besides, $C_{i,k}$ captures the costs of infection, including medical treatment expenditures, absence from work or reduced personal well-being. Finally, agents discount the payoffs of future events using a discount rate r , which is assumed to be constant.

Even though the actual infection probability $\lambda_k(t)$ is time dependent due to fluctuations in the incidence of the disease in the population, it is assumed to lie beyond the capabilities of any individual to simulate the entire social network for an accurate prediction of its evolution. Instead, each susceptible agent makes a point estimation $\hat{\lambda}_k$ and assumes it to be constant during the forward time-horizon T :⁶

$$\hat{\lambda}_k = \hat{\beta} \cdot \frac{n_k(t)}{n_{k,T}} = \beta \cdot \frac{n_k(t)}{n_{k,T}}, \quad (10)$$

where $n_{k,T}$ corresponds to the agent's total number of neighbours and $\hat{\beta}$ being an estimated probability of infection, based on knowledge of historical cases. Given the characteristics of the disease, the estimation of $\hat{\beta}$ is assumed to fit the actual β , thus $\hat{\beta} = \beta$. The hypothesis of making a point estimation that is constant during the forward time-horizon, amounts to treating the infection dynamics as a stationary Markov chain at the agent level:

$$\mathbf{x}_k(t+1) = \hat{\mathbf{Q}}_k \cdot \mathbf{x}_k(t), \quad (11)$$

⁶The heuristic approach for the calculation is justified on the basis of bounded rationality, given the outbreak characteristics of the disease. Especially, the following comes into play: While the disease percolates in the population, so does the knowledge about the disease. An agent is informed about the fact that a disease is spreading in the population as soon as any of the neighbours are infected, but cannot derive probabilities regarding spreading rate and severity. Given bounded rationality, the share of infected neighbours is the heuristic basis from which an agent derives the probability of infection.

with:

$$\hat{\mathbf{Q}}_k = \begin{pmatrix} 1 - \hat{\lambda}_k & 0 & 0 & 0 \\ \hat{\lambda}_k & 1 - \gamma_k & 0 & 0 \\ 0 & \gamma_k & 1 & 0 \\ 0 & 0 & 0 & 1 \end{pmatrix} \quad (12)$$

Given that the evolution of a stationary Markov chain is independent of any absolute time reference, without loss of generality (7) can be rewritten using $t = 0$. Employing (11) and (12):

$$U_k(\mathbf{x}_k(0), T) = \mathbf{f}_k(0) \cdot \mathbf{x}_k(0) + \sum_{t=1}^T \mathbf{f}_k(t) \cdot \left(\frac{\hat{\mathbf{Q}}_k}{1+r} \right)^t \cdot \mathbf{x}_k(0) \quad (13)$$

In order to compute the power $\hat{\mathbf{Q}}_k^t$, the matrix can be diagonalized:

$$\hat{\mathbf{Q}}_k = \hat{\mathbf{R}}_k \hat{\mathbf{\Lambda}}_k \hat{\mathbf{R}}_k^{-1} \quad (14)$$

And (13) can be rewritten as follows:

$$U_k(\mathbf{x}_k(0), T) = \left[\mathbf{f}_k(0) + \mathbf{f}_k(t) \cdot \hat{\mathbf{R}}_k \cdot \sum_{t=1}^T \left(\frac{\hat{\mathbf{\Lambda}}_k}{1+r} \right)^t \cdot \hat{\mathbf{R}}_k^{-1} \right] \cdot \mathbf{x}_k(0) \quad (15)$$

Finally, performing the required computations are obtained:

$$U_k(\mathbf{x}_k(0), T) = -p_{vacc} \cdot C_{v,k} - (1 - p_{vacc}) \cdot C_{notv,k} \quad (16)$$

where:

$$C_{notv,k} = C_{i,k} \cdot \left(\frac{\hat{\lambda}_k}{\gamma_k - \hat{\lambda}_k} \right) \cdot \left[\sum_{t=1}^T \left(\frac{1 - \hat{\lambda}_k}{1+r} \right)^t - \sum_{t=1}^T \left(\frac{1 - \gamma_k}{1+r} \right)^t \right] \quad (17)$$

Equation (16) is linear in p_{vacc} , so it has only one global maximum which depends on the relative cost of each decision. In particular, the preferred strategies are the following:

$$\begin{aligned} p_{vacc} &= 0, & \text{for } C_{v,k} > C_{notv,k} \\ p_{vacc} &= 1, & \text{for } C_{notv,k} > C_{v,k} \\ p_{vacc} &\in (0, 1), & \text{for } C_{v,k} = C_{notv,k} \end{aligned} \quad (18)$$

Thus, agents follow a pure strategy for almost all values of $C_{notv,k}$. Following equation (18), it becomes clear that *ceteris paribus* a different vaccination strategy will be chosen depending on an agent's beliefs, manifested through different relative values for $C_{v,k}$ and $C_{i,k}$. In particular, it is expected that individuals skeptical towards vaccines will preferentially decide not to vaccinate for a given $\hat{\lambda}_k$ and T , as they consider the costs to be higher than what individuals who believe in the effectiveness of vaccines do.

3.3 Network structure

The hierarchical configuration model in [Stegehuis et al. \(2016\)](#) provides an orientation for the model which is employed in this thesis. Adopting the two belief-groups, these are identified as sub-communities of the whole population. Each group is assumed to have a close intra-connection and a looser inter-connection. A small-world model is employed by formulating Watts-Strogatz networks [Watts and Strogatz \(1998\)](#) for every group, which are then connected as outlined below.

Each community $G \in \{T, S\}$ is a subset of the whole population N , $G \subset N$, with T representing 'trusters' and S representing 'skepticals'. Furthermore,

$$g: \mathbb{N} \rightarrow \{1, 2\}, g(i) \mapsto \begin{cases} 1, & i \text{ in group } T \\ 2, & i \text{ in group } S \end{cases} \quad (19)$$

indicates community-membership for an individual agent $i \in N$. The groups consist of a total of n_G members, according to $n_G = \sum_{i \in N} p_G(i) = p_G(i) * n$. With $n = \|N\|$ being the number of nodes in the total population N . Furthermore, $p_G(i)$ defines the probabilistic group allocation for a node i to be assigned to group $m \in \{1, 2\}$, such that

$$p_G(i) = \begin{cases} p_1, & i \text{ assigned to } T \\ 1 - p_1 =: p_2, & i \text{ assigned to } S \end{cases}, p_{1,2} \in [0, 1] \quad (20)$$

and $p_G(i)$ is independent of the individual agent i .

The Watts-Strogatz graph for every group $G \subset N$ is then built by taking into account $k(i)$, the number of nearest neighbours of i that i is connected to in a ring topology. Following, the network is adjusted by looping over the edges in each group, which are then rewired according to $p_{rew} \in (0, 1)$.

Thereafter, the two graphs are combined by adding an additional fraction of the edges in both groups for any two members $i, j \in N, i \neq j$, of different groups, requiring $g(i) \neq g(j)$. The amount of edges e_{add} is the fraction according to

$$e_{add} = a * e_G = a * \left(\sum_{i \in T} k(i) + \sum_{j \in S} k(j) \right), \quad (21)$$

with $a \in (0, 1)$, and

$$e_G = \left(\sum_{i \in T} k(i) + \sum_{j \in S} k(j) \right), \quad (22)$$

the total of edges in both groups. Any two members of different groups are then randomly connected until the amount of added connections reaches e_{add} .

4 Initial Setup and Baseline Parameters

The model described in the previous section contains a list of free parameters, whose baseline values are summarised in Table 1 below and are used in all simulations unless stated otherwise.

Parameter	Value
r	0.01
T	10 days
β	0.05 day^{-1}
γ	0.05 day^{-1}
$C_{i,T} = C_{i,S}$	1.0
$C_{v,T}$	0.01
$C_{v,S}$	0.05
k	8
α	0.3
$p_{rewiring}$	0.2

Table 1: Baseline values for the free parameters of the epidemic model

With respect to the parameters affecting each agent’s decision process, the value of γ is specified assuming that a seasonal infectious disease would take an average of 20 days to get recovered from, and T is chosen as 1/2 of this time frame. For the current implementation of the model, no dependency of γ on the agent state was included, so that $\forall k : \gamma_k = \gamma$. Given that the decision process is governed by the relative cost of vaccination to infection, the latter is fixed at a reference value of 1.0 for both groups and only C_v was set to reflect their different subjective costs. Finally, β was obtained from numerical experiments matching the expected dynamics for a fully connected graph, corresponding to a completely mixed population.

The parameters describing the network structure are set to describe a community of citizens in a typical urban environment. In this regard, a value of $k = 8$ is chosen for the number of nearest neighbours in both groups of affiliation as well as a fraction $\alpha = 0.3$ for the proportion of links between the two belief communities, in order to reflect differences in interpersonal affinity. The group population frequency q was set to 0.5 as a baseline in order to have an unbiased reference from which derive the sensitivity of the model output to variations in this parameter.

5 Implementation

All our calculations are carried out in Python. More specifically we used *networkx* for creating the network, *numpy* for calculations and *matplotlib* to visualize the results.

The code is split up in three files. *main.py* forms the core of the simulation and is the only file that should be executed. Also, all variables that characterize the simulation and can be altered in *main.py* to obtain different results.

5.1 Creating the network

By executing *main.py* an object of type *SmallWorldNetwork* (defined in *small_world_network.py*) is created. The parameters characterizing the network are *n*, *group_percentages*, *k*, *change_edge_percentage* and *alpha* defined at the beginning of *main.py*.

n defines the total number of nodes in the network. This number is then split up into different groups according to *group_percentages*. For example, if $n = 100$ and $group_percentages = [0.2, 0.8]$ two groups are created. One with 20 nodes and one with 80 nodes. For each of these groups a Watts-Strogatz model is created using *k* and *change_edge_percentage*. In a Watts-Strogatz model each node is connected to its *k* nearest neighbors. Then each edge is rewired with a probability of *change_edge_percentage*.

After creating a model for each group, the individual groups are loosely connected with a percentage *alpha*. In other words $alpha * n$ nodes are connected to both groups while all other nodes only share edges with nodes of the same group.

Thus, it is more likely to be connected to members of your own group but at the same time groups are never completely isolated from each other.

In a last step the created network is populated with agents. Hence, for each node an agent with the respective group type is created and stored in a list. The initial health status (susceptible, infected or vaccinated) is derived from rates defined in *lim_init_infected* and *lim_init_vacci*. Furthermore, each agent has a certain age that is derived from a normal distribution using *age_mu* and *age_sigma*.

Age is only included for possible extensions of the model in the future. It is not being used in our model.

5.2 Simulating the agents' behaviour

Almost all functions in *main.py* are responsible for visualizing the results. The simulation itself almost entirely takes place in the *Agent* class defined in *agent.py*.

In our case every iteration represents a day in the agents' life. The number of days to be simulated is defined by the variable *frames*. Hence, every day the main file loops over all agents in the network and thus calls the *run* function exactly once (per day). Starting from the *run* function a number of other functions is called that determine whether the agent is getting infected, recovers or vaccinates. For the decision of vaccination the *act* function gathers the different values needed in equation (16) to ultimately decide whether to vaccinate or not (equation (17)).

6 Simulation Results and Discussion

For a higher share of trusters in the population, the amount of vaccinated agents increases. This results is shown in [Figure 1a](#) and [Figure 2a](#) and is in line with previous findings. Furthermore, an increase in the share of trusters yields an even higher ratio of vaccinated trusters to vaccinated skepticals when a threshold value of around $p_T = 0.7$ is reached. With more trusters that the ratio sharply increases, which is shown in [Figure 1b](#) and [Figure 2b](#). Especially, for a higher connection percentage between the communities, an even higher ratio can be found. These findings can be explained along two lines. First, the vaccination ratio is higher in the truster community by design. Thus, a higher share of trusters and more vaccinated trusters face less vaccinated skepticals in general. Second, the more vaccinated trusters are present in a community, the lower is the incentive for skepticals to get vaccinated. Since the share increases, the incentive drops further and based on this free-riding behaviour, the ratio jumps even higher. For the case of the two communities being more closely connected, skepticals are on average surrounded by more vaccinated individuals and the ratio is larger for a higher connection probability α .

Analysing [Figure 3](#) and [Figure 4](#), it is shown that the uptake in vaccines resembles an s-curve. Also, the uptake lags both the increase in infections and the current number of infected, until this number peaks. By design, the outbreak is small at the beginning, so the incentive to vaccinated exists only for a few individuals, which allows the disease to spread particularly in the skeptical community. Regarding the dynamics, the number of vaccinated agents surpasses the number of current infectious cases for the models with $T < 10$, while the cases are mixed for $T = 10$, and for $T = 30$ the opposite appears. This is in line with the update times, which are quicker than the spread of the disease for $T = \{2, 5\}$ and slower for $T \geq 10$. Especially for $T = 30$, the update rate is too slow to keep pace with the disease spread and an overwhelming majority of the population gets infected during the epidemic season.

Regarding the cost-perspective, the employed model confirms findings of previous research and is in line with the theoretical model, since higher costs reduce the uptake levels for both communities. But comparing the effects of costs in [Figure 3](#) and [Figure 4](#) to the effects of different shares of trusters, cf. [Figure 1a](#) and [Figure 2a](#), in the community yields more remarkable results. The uptake levels are more sensitive to the share of trusters in the community, compared to the cost-ratios of the individual communities. Interesting are the cases of [Figure 3e](#) and [Figure 4a](#), where the costs are too low for the forecast-period. Thus, the vaccine uptake, for the agents facing a decision, overtakes the infections and the pandemic is contained. On the other hand, for [Figure 3h](#) and [Figure 4h](#), the costs are too high and the disease reaches an overwhelming majority of the population.

Furthermore, the cost sensitivities of both groups is confirmed in [Figure 5a](#)

and [Figure 5b](#). But of special interest is the following: In the truster community, agents are more likely to stay healthy throughout the outbreak, even if they do not vaccinate. While in the community of skeptical agents, this sort of free-riding behaviour does not pay off for the individual and results in most of the cases in getting infected. So even if the agent is willing to get vaccinated ('truster'), it might not be necessary at all if the neighbourhood consists mainly of agents that contribute to the prevention of the spread of the infection.⁷

Among the assumptions of our current model that restrict the extent to which our results can be extrapolated, is the statement that agents do not have memory of past infections in order to learn a strategy with a long-term higher payoff. This assumption is justified referring to an unexpected outbreak for which no previous experience can provide useful knowledge and/or immunity, in order to influence the decision of an agent to vaccinate. Therefore, the probability of infection is estimated exclusively through the current incidence of the disease in each neighbourhood. Nevertheless, it is realistic to expect for agents facing an outbreak of an infectious diseases like influenza to exploit their previous experiences of similar outbreaks in the form of a prior probability of getting infected, even if the strain is new and they lack immunity against it. One possible consequence of including this effect could be a higher baseline uptake for all behavioural groups, as the maximisation of expected utility would lean toward taking vaccines without the need for the buildup of a critical mass of infectious individuals to trigger it.

7 Summary and Outlook

Analysing the outbreak of an influenza strain in a population of two communities that differ with respect to their beliefs regarding vaccinations, the obtained results are in line with previous research and add further interesting findings. The model and simulations confirm the cost sensitivity of agents with regards to their vaccination decision. It is shown that the time-horizon, in terms of updating the individual decision, is crucial for the spread of an infectious disease. For agents that update frequently, an outbreak of disastrous size can be prevented, which is not the case for agents that rely on their initial decision for longer time-spans. Increasing the share of trusters in the community significantly contributes to the uptake levels of vaccinations. But especially, uptake levels are more sensitive to the share of trusters in the community, compared to the cost-ratios of the individual communities, which is of special interest for public health policies.⁸

The employed model serves as a baseline for future research on the effects of belief-groups on vaccination uptake in structured networks. Refinements along the following lines should provide further contributions to existing research:

⁷The dynamics of [Figure 5a](#) and [Figure 5b](#) are captured in mp4-files, which can be obtained from the github folders.

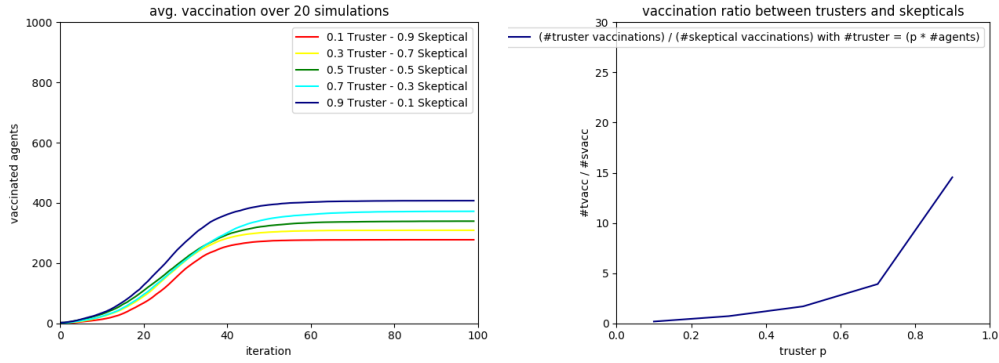
⁸As outlined in the Literature Review, compare [Shim et al. \(2012\)](#) and [Stegehuis et al. \(2016\)](#).

Regarding the agent perspective, it is either proposed to work with a non-binary coding of the groups, thus allowing for refined group-membership such that different beliefs and cost assumptions can be accounted for. Otherwise, changing the individual costs for infection or vaccination should result in changed SIVR-dynamics. In addition, the agents should be individualised to a more specific degree which adds more reality to the model. Especially, taking into account the age-structure of the population should result in different costs of both vaccination and infection, while it can be assumed that the disease-specific parameters change as well. The employed model assumes a population that stays constant. While deaths can be accounted for in the existing model, the case of including births adds a more dynamic component in the spread and the modelling of the disease. Another feature that would be added is the possibility of modelling endemic diseases.

Concerning the network perspective, analysing different network types will provide decisive results for early and targeted intervention measures in the public. Working with dynamic networks that change over time, due to general demographical dynamics or resulting from agents' behaviours, adds another feature that is valuable for future research.

Appendix

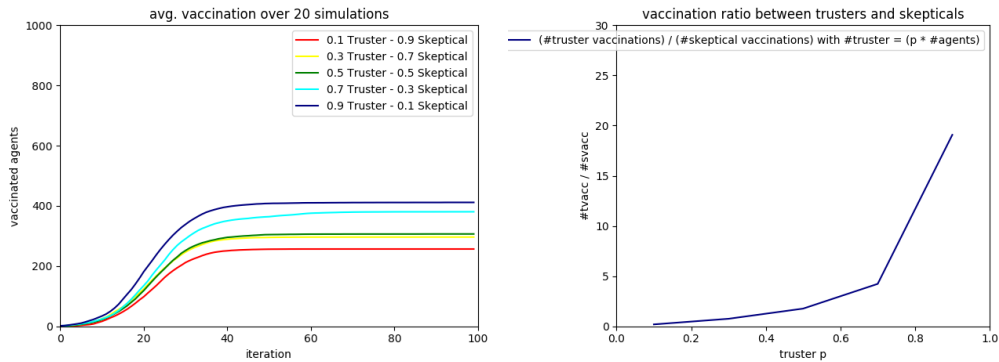
Figure 1: Average amount of vaccinated agents and vaccination ratio for various shares of 'trusters'.



(a) Average amount of vaccinated agents (b) Vaccination ratio trusters to skepticals

Figure 1: Average amount of vaccinated agents for shares of 'trusters': $\frac{n_T}{n} \in [0.1, 0.9]$. Averages are calculated over 20 simulations. Connection of groups with $\alpha = 0.05$

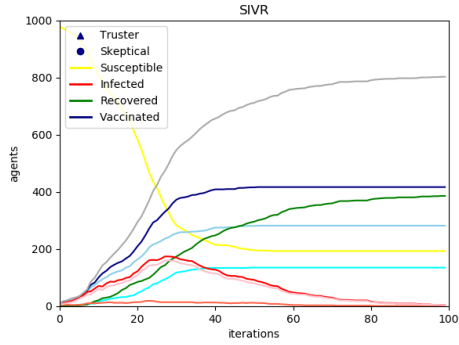
Figure 2: Average amount of vaccinated agents and vaccination ratio for various shares of 'trusters'.



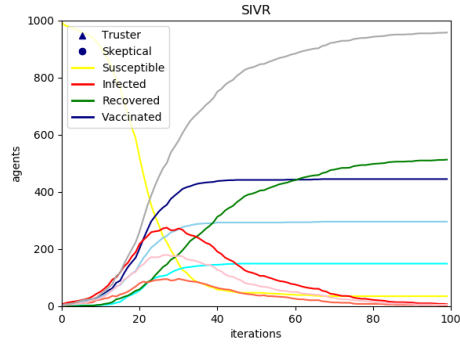
(a) Average amount of vaccinated agents (b) Vaccination ratio trusters to skepticals

Figure 2: Average amount of vaccinated agents for shares of 'trusters': $\frac{n_T}{n} \in [0.1, 0.9]$. Averages are calculated over 20 simulations. Connection of groups with $\alpha = 0.3$

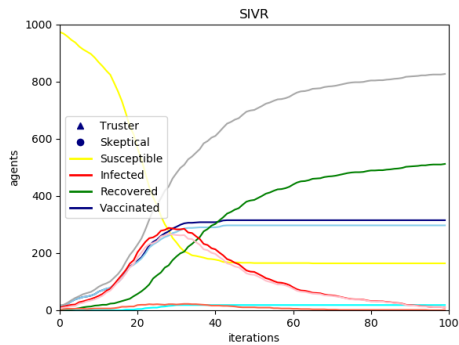
Figure 3: SIVR dynamics for different costs of vaccination and different time-horizons.



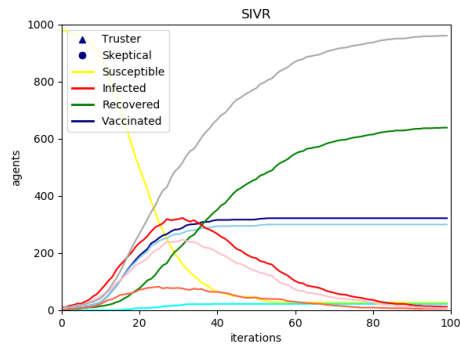
(a) $T = 2, C_{v,S} = 0.05, C_{v,T} = 0.01$



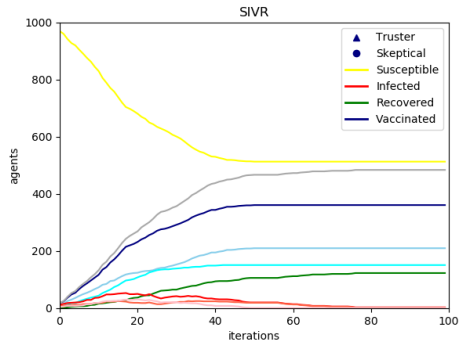
(b) $T = 2, C_{v,S} = 0.05, C_{v,T} = 0.02$



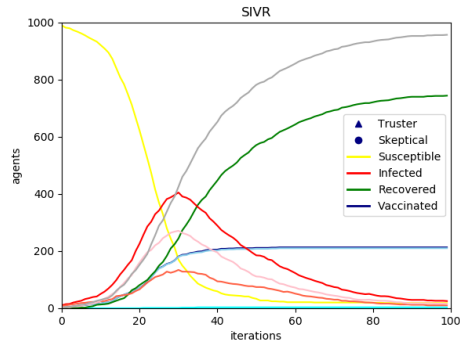
(c) $T = 2, C_{v,S} = 0.1, C_{v,T} = 0.01$



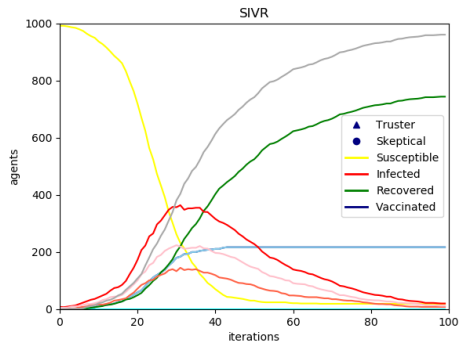
(d) $T = 2, C_{v,S} = 0.1, C_{v,T} = 0.02$



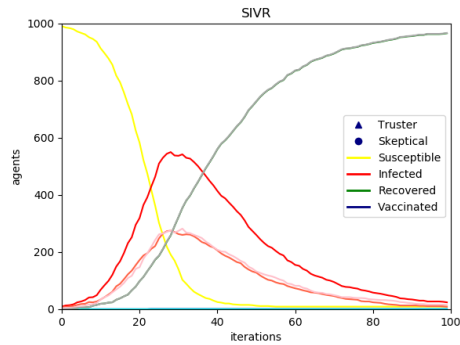
(e) $T = 5, C_{v,S} = 0.05, C_{v,T} = 0.01$



(f) $T = 5, C_{v,S} = 0.5, C_{v,T} = 0.1$



(g) $T = 5, C_{v,S} = 1.0, C_{v,T} = 0.1$



(h) $T = 5, C_{v,S} = 1.0, C_{v,T} = 0.5$

Figure 3: SIVR dynamics for different costs of vaccination and different time-horizons. Default parameters as follows: $C_{v,S} = 0.05, C_{v,T} = 0.01, p_{S,T} = 0.5, T = 5, \alpha = 0.3$. Deviations according to the respective caption.

Figure 4: SIVR dynamics for different costs of vaccination and different time-horizons.

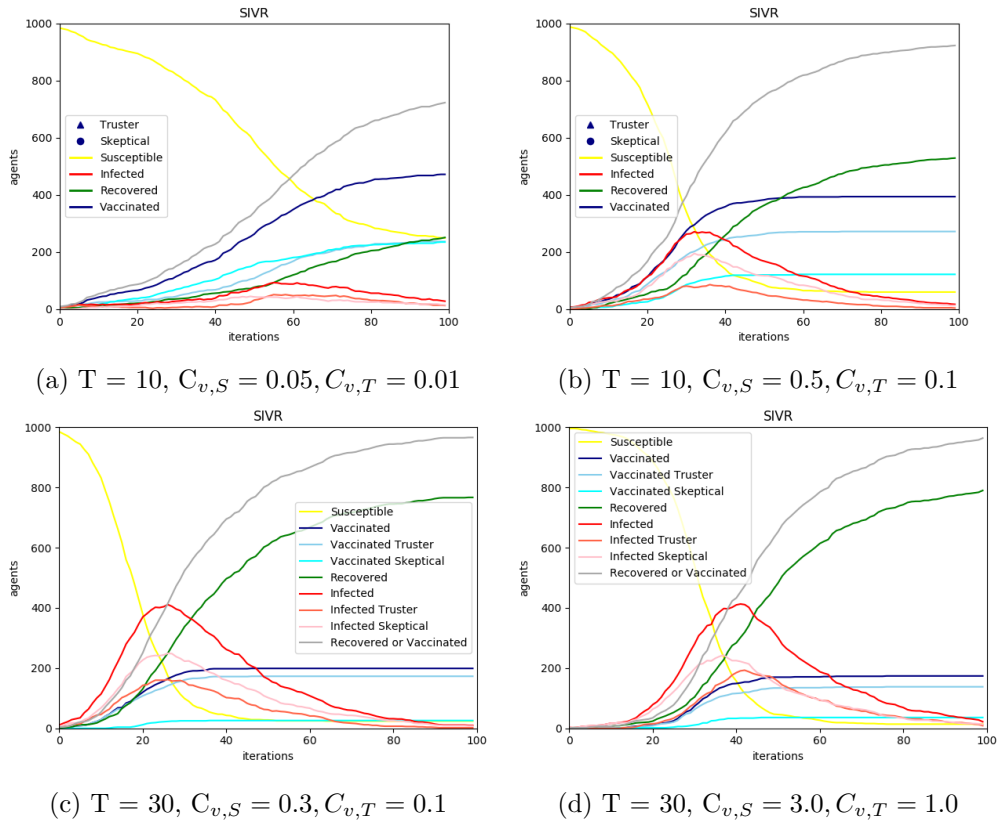


Figure 4: SIVR dynamics for different costs of vaccination and different time-horizons. Default parameters as follows: $C_{v,S} = 0.05, C_{v,T} = 0.01, p_{S,T} = 0.5, T = 5, \alpha = 0.3$. Deviations according to the respective caption.

Figure 5: SIVR dynamics for different costs of vaccination.

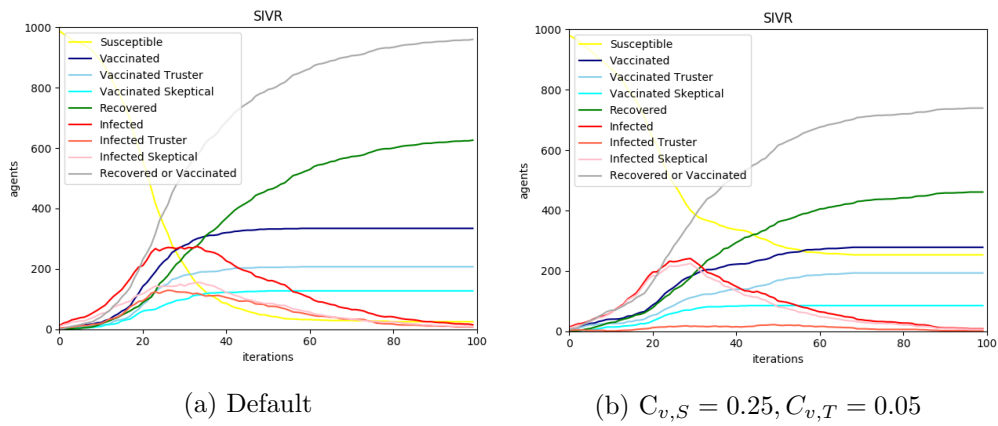


Figure 5: SIVR dynamics for different costs of vaccination. Default parameters as follows: $C_{v,S} = 0.2, C_{v,T} = 0.1, p_{S,T} = 0.5, T = 5, \alpha = 0.05$. Deviations according to the respective caption.

References

- Bauch, C. T. and Bhattacharyya, S. (2012), ‘Evolutionary game theory and social learning can determine how vaccine scares unfold’, *PLoS computational biology* **8**(4), e1002452.
- Bauch, C. T. and Earn, D. J. (2004), ‘Vaccination and the theory of games’, *Proceedings of the National Academy of Sciences* **101**(36), 13391–13394.
- Dadlani, A. (2013), ‘Deterministic models in epidemiology: from modeling to implementation’.
- Earn, D., Brauer, F., van den Driessche, P. and Wu, J. (2008), *Mathematical epidemiology*, Springer Berlin.
- Fu, F., Rosenbloom, D. I., Wang, L. and Nowak, M. A. (2010), ‘Imitation dynamics of vaccination behaviour on social networks’, *Proceedings of the Royal Society B: Biological Sciences* **278**(1702), 42–49.
- Hancock, K., Veguilla, V., Lu, X., Zhong, W., Butler, E. N., Sun, H., Liu, F., Dong, L., DeVos, J. R., Gargiullo, P. M. et al. (2009), ‘Cross-reactive antibody responses to the 2009 pandemic h1n1 influenza virus’, *New England Journal of Medicine* **361**(20), 1945–1952.
- Heesterbeek, H. (2005), ‘The law of mass-action in epidemiology: a historical perspective’, *Ecological paradigms lost: routes of theory change* pp. 81–104.
- Keeling, M. J. and Eames, K. T. (2005), ‘Networks and epidemic models’, *Journal of the Royal Society Interface* **2**(4), 295–307.
- Kermack, W. O. and McKendrick, A. G. (1927), ‘A contribution to the mathematical theory of epidemics’, *Proceedings of the royal society of london. Series A, Containing papers of a mathematical and physical character* **115**(772), 700–721.
- Liu, M., Li, D., Qin, P., Liu, C., Wang, H. and Wang, F. (2015), ‘Epidemics in interconnected small-world networks’, *PloS one* **10**(3), e0120701.
- Liu, X.-T., Wu, Z.-X. and Zhang, L. (2012), ‘Impact of committed individuals on vaccination behavior’, *Physical Review E* **86**(5), 051132.
- Meyers, L. A., Pourbohloul, B., Newman, M. E., Skowronski, D. M. and Brunham, R. C. (2005), ‘Network theory and sars: predicting outbreak diversity’, *Journal of theoretical biology* **232**(1), 71–81.
- Moore, C. and Newman, M. E. (2000), ‘Epidemics and percolation in small-world networks’, *Physical Review E* **61**(5), 5678.

- Neumann, G., Noda, T. and Kawaoka, Y. (2009), ‘Emergence and pandemic potential of swine-origin h1n1 influenza virus’, *Nature* **459**(7249), 931.
- Newman, M. E. and Watts, D. J. (1999), ‘Scaling and percolation in the small-world network model’, *Physical review E* **60**(6), 7332.
- Pastor-Satorras, R. and Vespignani, A. (2002), ‘Immunization of complex networks’, *Physical review E* **65**(3), 036104.
- Rusu, E. (2015), ‘Network models in epidemiology: Considering discrete and continuous dynamics’, *arXiv preprint arXiv:1511.01062* .
- Shi, B., Qiu, H., Niu, W., Ren, Y., Ding, H. and Chen, D. (2017), ‘Voluntary vaccination through self-organizing behaviors on locally-mixed social networks’, *Scientific reports* **7**(1), 2665.
- Shim, E., Grefenstette, J. J., Albert, S. M., Cakouros, B. E. and Burke, D. S. (2012), ‘A game dynamic model for vaccine skeptics and vaccine believers: measles as an example’, *Journal of Theoretical Biology* **295**, 194–203.
- Smith, G. J., Vijaykrishna, D., Bahl, J., Lycett, S. J., Worobey, M., Pybus, O. G., Ma, S. K., Cheung, C. L., Raghwani, J., Bhatt, S. et al. (2009), ‘Origins and evolutionary genomics of the 2009 swine-origin h1n1 influenza a epidemic’, *Nature* **459**(7250), 1122.
- Stegehuis, C., Van Der Hofstad, R. and Van Leeuwen, J. S. (2016), ‘Epidemic spreading on complex networks with community structures’, *Scientific reports* **6**, 29748.
- Sun, G.-Q., Jusup, M., Jin, Z., Wang, Y. and Wang, Z. (2016), ‘Pattern transitions in spatial epidemics: Mechanisms and emergent properties’, *Physics of life reviews* **19**, 43–73.
- Tornatore, E., Vetro, P. and Buccellato, S. M. (2014), ‘Sivir epidemic model with stochastic perturbation’, *Neural Computing and Applications* **24**(2), 309–315.
- Watts, D. J. and Strogatz, S. H. (1998), ‘Collective dynamics of ‘small-world’ networks’, *nature* **393**(6684), 440.
- Wilson, E. B. and Worcester, J. (1945), ‘The law of mass action in epidemiology’, *Proceedings of the National Academy of Sciences of the United States of America* **31**(1), 24.